Journal of Engineering and Applied Research (JEAR)

National University of Skills

Summer & Autumn 2025, Vol. 2, No. 2, p. 161- 183

Journal Homepage: https://jear.tvu.ac.ir

:10.48301/JEAR.2024.474745.1041

Investigation of Von Karman rectangular plates nonlinear vibration : Optimal Ho-motopy Analysis Method

Mohammad Ali Kazemi[1*], Milad Fallahian[2], Seyed sajad Jafari[3], Amir Khaledian[4]

[1] Assistant Professor Department of Mechanical Engineering, Technical and Vocational University (TVU), Tehran, Iran

[2] Young Researchers & Elite Club, Hamedan Branch, Islamic Azad University, Hamedan, Iran

[3] Assistant Professor Department of Mechanical Engineering, Hamedan University of Technology, Hamedan, Iran

[4] Department of Electrical Engineering, Technical and Vocational University (TVU), Tehran, Iran

ARTICLE INFO

Article Type:
Original Research

Received: 09.13.2024
Revised: 12.07.2024
Accepted: 12.30.2024

Keyword:
Nonlinear vibration
Rectangular plate
Time function
Optimal Homotopy Analysis Method (OHAM)

***Corresponding Author:**
Mohammad Ali Kazemi
Email:
m-kazemi@tvu.ac.ir

ABSTRACT

In the present study, the Optimal Homotopy Analysis Method (OHAM) is utilized to analytically solve the nonlinear vibration equation of an isotropic rectangular plate considering shear deformation and rotary inertia effects based on the Von Karman theory. The accuracy of the OHAM results is validated through comparison with both previously published analytical studies and numerical solutions obtained using the bvp function in Maple, showing excellent agreement. The inclusion of a second auxiliary parameter in OHAM improves the convergence rate and extends the linear region of the solution curve. The influence of several system parameters, such as geometric ratios, initial amplitude, and damping characteristics, on the vibration amplitude and frequency response is investigated in detail. Furthermore, various mode shapes of the plate corresponding to different physical conditions are illustrated, clearly demonstrating the robustness, accuracy, and computational efficiency of the proposed analytical approach in reliably handling highly complex and nonlinear vibration problems.

E-ISSN: 3060-6357

Introduction

Plates are important role in engineering applications so that they are used in aircraft structures, nuclear vessels and etc. because of exposing to dynamic forces the nonlinear vibration of plates is an significant area of applied [1].

Scientists employ different methods including numerical, analytical and approximation methods to explore the nonlinear vibration of plates and beams [2-4]. Simply supported shear deformable cross-ply laminated plate was selected to study by Huang and Shen [5]. They probed the nonlinear free and forced vibrations and dynamic responses with piezoelectric actuators via an improved perturbation technique with assuming mechanical, electrical and thermal loads. Singha and Daripa [6] used the FEM to investigate large amplitude free vibration behavior of symmetrically laminated composite skew plates with considering the effects of shear deformation, in-plane and rotary inertia.

Heat conduction and temperature-dependent material properties are taken into attention in the analysis of nonlinear vibration and dynamic response in graded material plates in thermal environments by Huang and Shen [7] via improved perturbation technique. To find the free vibration frequencies and the mode shapes of plates, thick, circular and annular, a three dimensional analysis was performed by Kang [8] via Ritz method. Nonlinear thickness variation was assumed along the radial direction. Amabili [9] used three different boundary conditions in nonlinear vibration of rectangular plates and verified with experiment for large-amplitude vibrations around the fundamental resonance of the aluminum plate.

Nonlinear vibration in circular plate with variable thickness was solved by Ye [10] via Runge-Kutta method for two different boundary conditions, the clamped edge and the supported edge, with Maple V. Shen et al [11] studied nonlinear vibration for simply supported, rectangular, single layer graphene plate, considering the thermal effects and obtaining the material properties from molecular dynamics simulations. Nonlinear free vibration of functionally graded sector plates, which were made out of three types of graded materials were analyzed by Belalia and Houmat [12] with finite element method. Skew and trapezoidal Mindlin plates for nonlinear free and forced vibration by the use of a trapezoidal hierarchical finite element were analyzed by Leung and Zhu [13].

Also other researchers used different methods to investigate plate vibrations like differential quadrature method in laminated composite skew thin plates [14] and Reinforced Composite Functionally Graded Plates[15] and functionally graded variable thickness carbon nanotube annular plates[16], nonlinear finite element model analysis of a laminated composite plate [17] and thin rectangular plate [18] , Galerkin and Runge–Kutta method in initially stressed laminated plate [19] and impact on CNTRC plates[20], perturbation analysis on thin CFRPs woven laminated plates [21]

and etc. Liao and Marinca and Herisanu used Homotopy Analysis Method (HAM) for offering a general analytic method [22-24].

Yongqiang et al [25] presented a solution for free vibrations of the symmetric rectangular honeycomb sandwich panels via HAM. Fooladi et al [26] used HAM solution of kirchhoff simplified model for beam. Jafari et al [27] used HAM and DTM for the vibration of Euler-Bernoulli beams. In addition to the mentioned above applications, HAM can be also employed in other parts like fluid dynamics and etc [28-34]

To accelerate solution convergence, HAM with two auxiliary parameters was applied to investigate the nonlinear vibration of a rectangular plate. The second auxiliary parameter increases the rate of convergence [35-37]. In addition, the system parameters effects on the amplitude of oscillation are displayed and different mode shapes of the oscillation for various plate parameters are illustrated.

Problem definition

Figure 1 shows the dimension of a rectangular plate. The plate experiences large deflection and also it has unknown displacements. The displacement relations based on Von Karman theory are obtained:

$$u(x,y,z,t) = u_0(x,y,t) + z\,\alpha(x,y,t), \tag{1}$$

$$v(x,y,z,t) = v_0(x,y,t) + z\,\beta(x,y,t), \tag{2}$$

$$w(x,y,z,t) = w_0(x,y,t), \tag{3}$$

where u, v and w are the displacement components in the directions of x, y and z, respectively. Further, u_0, v_0 and w_0 are the mid-plane displacements. α and β are the angles between the normal to mid-plane before and after deformation, respectively.

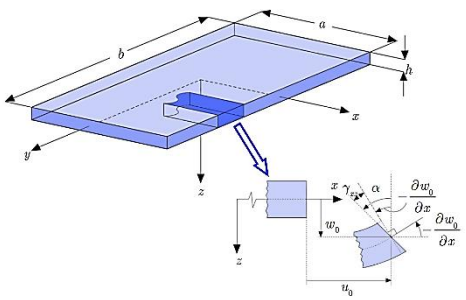

Figure 1. Configuration of the rectangular isotropic plate.

The Stress have five components as below:

$$\sigma_x = \frac{N_x}{h} + \frac{M_x}{I} = \frac{N_x}{h} + \frac{12M_x}{h^3}, \tag{4}$$

$$\sigma_y = \frac{N_x}{h} + \frac{M_y}{I} = \frac{N_y}{h} + \frac{12M_y}{h^3}, \tag{5}$$

$$\sigma_{xy} = \frac{N_{xy}}{h} + \frac{M_{xy}}{I} = \frac{N_{xy}}{h} + \frac{12M_{xy}}{h^3}, \tag{6}$$

$$\tau_{xz} = \frac{3}{2}\frac{Q_x}{h}\left(1 - 4\frac{Z^2}{h^2}\right), \tag{7}$$

$$\tau_{yz} = \frac{3}{2}\frac{Q_y}{h}\left(1 - 4\frac{Z^2}{h^2}\right), \tag{8}$$

where N is the membrane in-plane force, M is the bending moment, and Q is the internal shear force that are clearly shown in Figure 2. By considering the first order shear deformation theory and variation calculus the force-displacement relations for an elastic isotropic plate are obtained:

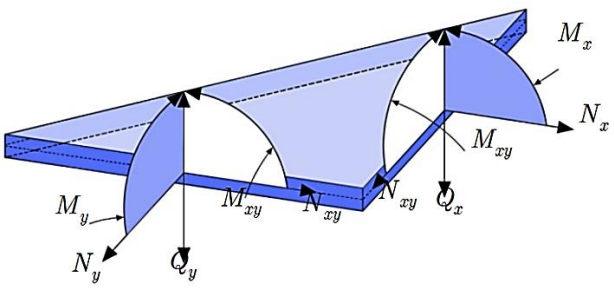

Figure 2. Plate's internal forces and bending moment.

It is easily obtained the following equations by calculating the kinetic and potential energy as well as using the Hamilton principle for conservative systems:

$$\frac{\partial M_x}{\partial x}+\frac{\partial M_{xy}}{\partial y}-Q_x=\frac{\rho h^3}{12}\alpha_{tt}, \tag{9}$$

$$\frac{\partial M_y}{\partial y}+\frac{\partial M_{xy}}{\partial x}-Q_y=\frac{\rho h^3}{12}\beta_{tt}, \tag{10}$$

$$\frac{\partial N_x}{\partial x}+\frac{\partial N_{xy}}{\partial y}=\rho\, h\, u_{tt}, \tag{11}$$

$$\frac{\partial N_y}{\partial y}+\frac{\partial N_{xy}}{\partial x}=\rho\, h\, v_{tt}, \tag{12}$$

$$\begin{aligned}&\frac{\partial N_x}{\partial x}w_x+N_x\frac{\partial^2 w}{\partial x^2}+\frac{\partial N_y}{\partial y}w_y+N_y\frac{\partial^2 w}{\partial y^2}+\frac{\partial N_{xy}}{\partial x}w_y\\&+\frac{\partial N_x y}{\partial y}w_x+2N_{xy}\frac{\partial^2 w}{\partial x\partial y}+\frac{\partial Q_x}{\partial x}+\frac{\partial Q_y}{\partial y}=\rho\, h\, w_{tt},\end{aligned} \tag{13}$$

The boundary conditions, obtained from the Hamilton principle, are as follows:

at $x=0$ and $x=a$:

$$u=0, \text{or} N_x=0, \tag{14}$$

$$v=0, \text{or} N_{xy}=0, \tag{15}$$

$$w=0, \text{or} Q_x+N_x\frac{\partial w}{\partial x}+N_{xy}\frac{\partial w}{\partial y}=0, \tag{16}$$

$$\alpha=0, or M_x=0, \tag{17}$$

$$\beta=0, \text{or} M_{xy}=0, \tag{18}$$

and at $y=0$ & $y=b$:

$$u=0, \text{or} N_{xy}=0, \tag{19}$$

$$v=0, \text{or} N_y=0, \tag{20}$$

$$w=0, \text{or} Q_y+N_{xy}\frac{\partial w}{\partial x}+N_y\frac{\partial w}{\partial y}=0, \tag{21}$$

$$\alpha=0, \text{or} M_{xy}=0, \tag{22}$$

$$\beta=0, \text{or} M_y=0, \tag{23}$$

It is possible to assume that transverse motion occurs basically. An Airy stress function φ can be introduced as follows:

$$N_x = \frac{\partial^2 \varphi}{\partial y^2}, \tag{24}$$

$$N_y = \frac{\partial^2 \varphi}{\partial x^2}, \tag{25}$$

$$N_{xy} = -\frac{\partial^2 \varphi}{\partial x \partial y}, \tag{26}$$

By Substituting the airy stress functions in the motion equations:

$$D\frac{\partial^2 \alpha}{\partial x^2} + \frac{D(1-\nu)}{2}\frac{\partial^2 \alpha}{\partial y^2} + \frac{D(1+\nu)}{2}\frac{\partial^2 \beta}{\partial x \partial y} - \frac{5Eh}{12(1+\nu)}\left(\alpha + \frac{\partial w}{\partial x}\right) - \frac{\rho h^3}{12}\alpha_{tt} = 0, \tag{27}$$

$$D\frac{\partial^2 \beta}{\partial y^2} + \frac{D(1-\nu)}{2}\frac{\partial^2 \beta}{\partial x^2} + \frac{D(1+\nu)}{2}\frac{\partial^2 \alpha}{\partial x \partial y} - 5\frac{Eh}{12(1+\nu)}\left(\beta + \frac{\partial w}{\partial y}\right) - \frac{\rho h^3}{12}\beta_{tt} = 0, \tag{28}$$

$$\frac{\partial^2 \varphi}{\partial x^2}\frac{\partial^2 w}{\partial y^2} + \frac{\partial^2 \varphi}{\partial y^2}\frac{\partial^2 w}{\partial x^2} - 2\frac{\partial^2 \varphi}{\partial x \partial y} + \frac{5Eh}{12(1+\nu)}\left(\frac{\partial \alpha}{dx} + \frac{\partial \beta}{dy} + \nabla^2 w\right) - \rho\, h\, w_{tt} = 0, \tag{29}$$

for the middle surface strains the proper compatibility equation must be considered as below [38]:

$$\nabla^4 \varphi = Eh\left[\left(\frac{\partial^2 w}{\partial x \partial y}\right)^2 - \frac{\partial^2 w}{\partial x^2}\frac{\partial^2 w}{\partial y^2}\right], \tag{30}$$

Eliminating α and β from the above equations, one can derive the following equation (the motion equation in the transverse direction for a rectangular isotropic elastic plate):

$$\left[\frac{D^2(1-\nu)}{2}\nabla^4 - \frac{D\rho h^3(3-\nu)}{24}\nabla^2\frac{\partial^2}{\partial t^2} - \frac{5D\,E\,h\,(3-\nu)}{24\,(1+\nu)}\nabla^2 + \frac{25E^2h^2}{144\,(1+\nu)^2} + \frac{5\rho E h^4}{72\,(1+\nu)}\frac{\partial^2}{\partial t^2}\right]\times \left[\frac{\partial^2 \varphi}{\partial x^2}\frac{\partial^2 w}{\partial y^2} + \frac{\partial^2 \varphi}{\partial y^2}\frac{\partial^2 w}{\partial x^2} - 2\frac{\partial^2 \varphi}{\partial x \partial y}\frac{\partial^2 w}{\partial x \partial y} + \frac{5\,E\,h}{12\,(1+\nu)}\nabla^2 w - \rho\, h\, \ddot{w}\right] + \frac{5\,E\,h}{12\,(1+\nu)}\left[\frac{5\,D\,E\,h}{24}\frac{(1-\nu)}{(1+\nu)}\nabla^4 - \frac{25E^2h^2}{144(1+\nu)^2}\nabla^2 - \frac{5\rho E h^4}{144\,(1+\nu)}\frac{\partial^2}{\partial t^2}\right]w = 0, \tag{39}$$

In the above equation $D = \frac{Eh^3}{12(1-\nu^2)}$. Without considering the effect of shear deformation and rotary inertia, the classical plate theory (CPT) is derived as Eq. (40):

$$\left[D\nabla^4 + \rho h\frac{\partial^2}{\partial t^2} - \frac{\partial^2\varphi}{\partial x^2}\frac{\partial^2}{\partial x^2} - \frac{\partial^2\varphi}{\partial y^2}\frac{\partial^2}{\partial y^2} - 2\frac{\partial^2\varphi}{\partial x\partial y}\frac{\partial^2}{\partial x\partial y}\right]w = 0, \tag{31}$$

The Airy stress function (φ), defined in Eqs. (24)-(26), is to satisfy the Eq. (30). Based on the definition of Airy stress function, the general boundary condition of the plate can be presented as:

$$u_0 = \int_{-a/2}^{+a/2}\left[\frac{1}{E\,h}\left(\frac{\partial^2\varphi}{\partial y^2} - \nu\frac{\partial^2\varphi}{\partial x^2}\right) - \frac{1}{2}\left(\frac{\partial w_0}{\partial x}\right)^2\right]dx = 0, \text{or} N_x = \frac{\partial^2\varphi}{\partial y^2} = 0, \tag{32}$$

$$v_0 = \int_{-b/2}^{+b/2}\left[\frac{1}{E\,h}\left(-\nu\frac{\partial^2\varphi}{\partial y^2} + \frac{\partial^2\varphi}{\partial x^2}\right) - \frac{1}{2}\left(\frac{\partial w_0}{\partial y}\right)^2\right]dx = 0, \text{or} N_{xy} = \frac{\partial^2\varphi}{\partial x\partial y} = 0, \tag{33}$$

$$w_0 = 0, \text{or} K\,G\,h\left(\frac{\partial w_0}{\partial x} + \alpha\right) + \frac{\partial^2\varphi}{\partial y^2}\frac{\partial w_0}{\partial x} - \frac{\partial^2\varphi}{\partial x\partial y}\frac{\partial w_0}{\partial y} = 0, \tag{34}$$

$$\alpha = 0, \text{or} M_x = \frac{\partial\alpha}{\partial x} + \nu\,\frac{\partial\beta}{\partial y} = 0, \tag{35}$$

$$\beta = 0, \text{or} M_{xy} = \frac{\partial\alpha}{\partial y} + \frac{\partial\beta}{\partial x} = 0, \tag{36}$$

at $y = -\frac{b}{2}$ & $y = \frac{b}{2}$:

$$u_0 = \int_{-a/2}^{+a/2}\left[\frac{1}{E\,h}\left(\frac{\partial^2\varphi}{\partial y^2} - \nu\frac{\partial^2\varphi}{\partial x^2}\right) - \frac{1}{2}\left(\frac{\partial w_0}{\partial x}\right)^2\right]dx = 0, \text{or} N_{xy} = \frac{\partial^2\varphi}{\partial x\partial y} = 0, \tag{37}$$

$$v_0 = \int_{-b/2}^{+b/2}\left[\frac{1}{E\,h}\left(-\nu\frac{\partial^2\varphi}{\partial y^2} + \frac{\partial^2\varphi}{\partial x^2}\right) - \frac{1}{2}\left(\frac{\partial w_0}{\partial y}\right)^2\right]dx = 0, \text{or} N_y = \frac{\partial^2\varphi}{\partial x^2} = 0, \tag{38}$$

$$w_0 = 0, \text{or} K\,G\,h\left(\frac{\partial w_0}{\partial y} + \beta\right) - \frac{\partial^2\varphi}{\partial x\partial y}\frac{\partial w_0}{\partial x} - \frac{\partial^2\varphi}{\partial x^2}\frac{\partial w_0}{\partial y} = 0, \tag{39}$$

$$\alpha = 0, \text{or} M_{xy} = \frac{\partial\alpha}{\partial y} + \frac{\partial\beta}{\partial x} = 0, \tag{40}$$

$$\beta = 0, \text{or} M_y = \nu\frac{\partial\alpha}{\partial x} + \frac{\partial\beta}{\partial y} = 0, \tag{41}$$

For more information about the procedure to obtain the Eqs. (32)-(41), please see [1]. The transverse mode shapes of the system are obtained by solving the Eq. **Error! Reference source not found.**. By considering movable simply supported the boundary condition equations are:

at $x = -a/2$ and $x = a/2$:

$$u_0 = \int_{-a/2}^{+a/2} \left[\frac{1}{E\,h}\left(\frac{\partial^2\varphi}{\partial y^2} - v\frac{\partial^2\varphi}{\partial x^2}\right) - \frac{1}{2}\left(\frac{\partial w_0}{\partial x}\right)^2\right] dx = 0, \text{or} N_x = \frac{\partial^2\varphi}{\partial y^2} = 0, \quad (51)$$

$$v_0 = \int_{-b/2}^{+b/2} \left[\frac{1}{E\,h}\left(-v\frac{\partial^2\varphi}{\partial y^2} + \frac{\partial^2\varphi}{\partial x^2}\right) - \frac{1}{2}\left(\frac{\partial w_0}{\partial y}\right)^2\right] dx = 0, \text{or} N_{xy} = \frac{\partial^2\varphi}{\partial x\partial y} = 0, \quad (52)$$

$$w_0 = 0, \quad (53)$$

$$M_{xy} = \frac{\partial\alpha}{\partial y} + \frac{\partial\beta}{\partial x} = 0, \quad (54)$$

$$\beta = 0, \quad (55)$$

at $y = -b/2$ & $y = b/2$:

$$u_0 = \int_{-a/2}^{+a/2} \left[\frac{1}{E\,h}\left(\frac{\partial^2\varphi}{\partial y^2} - v\frac{\partial^2\varphi}{\partial x^2}\right) - \frac{1}{2}\left(\frac{\partial w_0}{\partial x}\right)^2\right] dx = 0, \text{or} N_{xy} = \frac{\partial^2\varphi}{\partial x\partial y} = 0, \quad (56)$$

$$v_0 = \int_{-b/2}^{+b/2} \left[\frac{1}{E\,h}\left(-v\frac{\partial^2\varphi}{\partial y^2} + \frac{\partial^2\varphi}{\partial x^2}\right) - \frac{1}{2}\left(\frac{\partial w_0}{\partial y}\right)^2\right] dx = 0, \text{or} N_y = \frac{\partial^2\varphi}{\partial x^2} = 0, \quad (57)$$

$$w_0 = 0, \quad (58)$$

$$\alpha = 0, \quad (59)$$

$$M_y = v\frac{\partial\alpha}{\partial x} + \frac{\partial\beta}{\partial y} = 0, \quad (60)$$

Using the Galerkin method, explained in detail by Rashidi et al [1], the non-dimensional equation is obtained in the form of:

$$a_1 f^3 + a_2 f + a_3 f'' + a_4 f^2 f'' + a_5 f(f')^2 = 0, \quad (42)$$

where $r = h/a$ and

$$a_1 = \frac{\pi^8 r^6}{2304}\frac{(3-\nu)}{(1-\nu^2)^2} + \frac{5\pi^6(3-\nu)^2 r^4}{4608(1-\nu^2)^2} + \frac{25\pi^4 r^2(3-\nu)}{4608(1+\nu^2)(1-\nu)}, \quad (43)$$

$$a_2 = \frac{5\pi^6 r^4}{1728(1+\nu)^2(1-\nu^2)} + \frac{25\pi^4 r^2}{1728(1+\nu)^2(1-\nu^2)}, \quad (44)$$

$$a_3 = \frac{\pi^4 r^4}{1728(1+\nu)^2(1-\nu^2)} + \frac{5\pi^2 r^2(23-11\nu)}{3456(1+\nu)(1-\nu^2)} + \frac{25}{576(1+\nu)^2}, \quad (45)$$

$$a_4 = \frac{\pi^6 r^6(3-\nu)^2}{1536(1-\nu)(1-\nu^2)} + \frac{5\pi^4 r^4(3-\nu)}{768(1-\nu^2)}, \quad (46)$$

$$a_5 = \frac{\pi^6 r^6(3-\nu)^2}{768(1-\nu)(1-\nu^2)} + \frac{5\pi^4 r^4(3-\nu)}{384(1-\nu^2)}, \quad (47)$$

subject to the following boundary conditions:

$$f(0) = amp, f'(0) = 0, \quad (48)$$

The first term of Eq. (42) shows the nonlinearity in the stiffness and the last two terms are the nonlinear terms in inertia.

Solution by Optimal Homotopy Analysis Method

Consider the suitable initial approximation, due to the boundary conditions and the rule of solution expression

It is important to mention that α is the second auxiliary parameter, which is used to accelerate the convergence of the series. The auxiliary linear operator $\mathcal{L}_f(f)$ becomes:

$$\mathcal{L}_f(f) = \frac{\partial^2 f}{\partial \eta^2} + \alpha^2 f, \quad (69)$$

which the following property is satisfied

$$\mathcal{L}_f\big(c_1 \sin(\alpha x) + c_2 \cos(\alpha x)\big) = 0, \quad (70)$$

where c_i, $i = 1-2$,are the arbitrary constants. According to the Eq. (61), the nonlinear operator is introduced as

$$\mathcal{N}_f\big[\hat{f}(t;\, p)\big] = a_1 \hat{f}(t;\, p)^3 + a_2 \hat{f}(t;\, p) + a_3 \frac{\partial^2 \hat{f}(t;\, p)}{\partial t^2} + a_4 \hat{f}(t;\, p)^2 \frac{\partial^2 \hat{f}(t;\, p)}{\partial t^2} + a_5 \hat{f}(t;\, p) \left(\frac{\partial \hat{f}(t;\, p)}{\partial t}\right)^2, \quad (71)$$

where $p \in [0,1]$, is the embedding parameter. The zero-thorder deformation equation is formed as

$$(1-p)\mathcal{L}_f\big[\hat{f}(t;\, p) - f_0(t)\big] = p\hbar \mathcal{H}_f(t) \mathcal{N}_f\big[\hat{f}(t;\, p)\big], \quad (72)$$

where $\hbar$, is auxiliary nonzero parameter and the auxiliary function $\mathcal{H}_f(t)$ is selected

as

$$\mathcal{H}_f(t) = 1. \tag{73}$$

subject to the boundary conditions

$$\hat{f}(0;p) = amp, \qquad \frac{d\hat{f}(0;p)}{dt} = 0, \tag{74}$$

It is obvious that when $p$enhances from 0 to 1, $\hat{f}(t;\ p)$ varies from $f_0(t)$ to $f(t)$. Finally by the Taylor's theorem, we obtain

$$\hat{f}(t;\ p) = f_0(t) + \sum_{m=1}^{\infty} f_m(t)\, p^m, \tag{75}$$

where

$$f_m(t) = \frac{1}{m!}\frac{\partial^m \hat{f}(t;\ p)}{\partial p^m}\bigg|_{p=0}, \tag{76}$$

The convergence of the series (75) is strongly depended on the auxiliary parameter [22]. Assume $\hbar$ is chosen such that the series of Eq. (75) is convergent at $p = 1$, we have

$$f(t) = f_0(t) + \sum_{m=1}^{\infty} f_m(t), \tag{77}$$

Due to mth-order deformation equation, differentiating Eq (72) $m$times with respect to p and dividing by $m!$ at $p = 0$, we have:

$$\mathcal{L}_f[f_m(t) - \chi_m\ f_{m-1}(t)] = \hbar\, \mathcal{H}_f(t) R_{f,m}(t), \tag{78}$$

where

$$\begin{aligned} R_{f,m}(t) = a_1 \sum_{j=0}^{n-1}\left(f_{n-1-j}(t)\sum_{i=0}^{j}\left(f_i(t)f_{j-i}(t)\right)\right) + a_2 f_{n-1} + a_3\frac{\partial^2 f_{n-1}(t)}{\partial t^2} + \\ a_4 \sum_{j=0}^{n-1}\left(\frac{\partial^2 f_{n-1-j}(t)}{\partial t^2}\sum_{i=0}^{j}\left(f_i(t)f_{j-i}(t)\right)\right) + a_5 \sum_{j=0}^{n-1}\left(f_{n-1-j}(t)\sum_{i=0}^{j}\left(\frac{\partial f_i(t)}{\partial t}\frac{\partial f_{j-i}(t)}{\partial t}\right)\right), \end{aligned} \tag{79}$$

and

$$\chi_m = \begin{cases} 0, & m \le 1, \\ 1, & m > 1. \end{cases} \tag{80}$$

With respect to the following boundary conditions

$$f_m(0) = amp, \qquad \frac{df_m(0)}{dt} = 0, \tag{81}$$

The symbolic software MATHEMATICA is applied to solve the nonlinear equation, Eq. (78) with the boundary conditions (81), one after the other in the order of $m = 1,2,3,\ldots$

$$f_1(t) = \frac{1}{16\alpha^2}\left\{amp\ h\ sin(\alpha t)\left\langle 2t\alpha(4a_2 + 3a_1 amp^2 + (-4a_3 + (-3a_4 + \right.\right. \tag{82}$$
$$+amp^2(a_1 - (a_4 + a_5)\alpha^2)sin(2\alpha t)$$
$$\vdots$$

The convergence of the series of Eq. (75) forcefully hinges on the auxiliary parameter. The $\hbar-$curve of $f''(0)$, obtained by the different orders of approximation, is illustrated in Figure 3. In order to find the optimal value of $\hbar$, the residual error is displayed by Eq. (83). The residual errors for third order of approximation of Eq. (83) are shown in Figurs 4-5. The results display that the amount of error is shown to increase when the initial amplitude is increased.

$$\mathrm{Res}_f = a_1\, f(t)^3 + a_2\, f(t) + a_3\, \frac{d^2 f(t)}{dt^2} + a_4\, f(t)^2 \frac{d^2 f(t)}{dt^2} + a_5\, f(t) \left(\frac{df(t)}{dt}\right)^2, \tag{83}$$

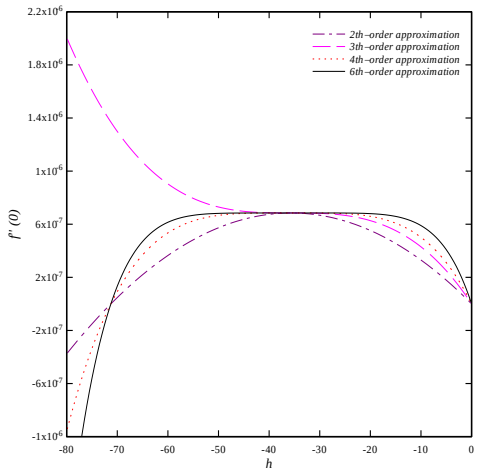

Figure 3. The $\hbar-$curve of $f''(0)$ obtained by different orders of approximation of HAM when $\nu = 0.3, r = 0.1$, $f(0) = 0.0002$, and $\alpha = 0.575$.

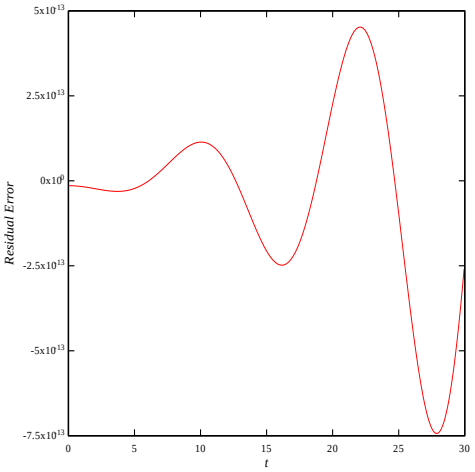

Figure 4. The residual error for Eq. (83) using third order of approximations when $\nu = 0.3, r = 0.1, f(0) = 0.0002$, and $\alpha = 0.575$.

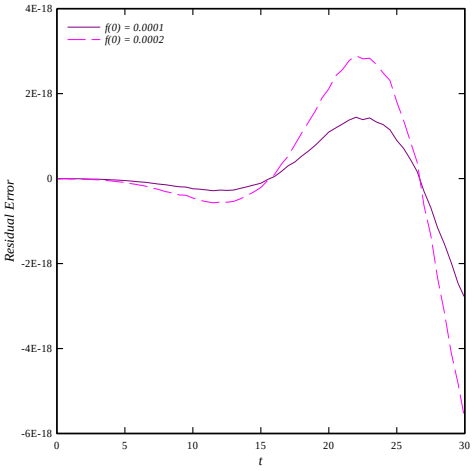

Figure 5. The residual error for Eq. (83) using third order of approximations for different initial amplitude when $\nu = 0.5, r = 0.05$ and $\alpha = 0.325$.

Results and Discussions

Graphical representation of results is very effective to illustrate the efficiency and accuracy of the HAM solution. In order to highlight the validity of the analytical method which is used in this research, we compare our results with the numerical

solutions obtained by using bvp function from Maple and the results of homotopy perturbation method (HPM) which are presented by Rashidi et al [1]. A very good agreement can be observed between them. It is important to note that the second auxiliary parameter is applied to increase the straight line region of $\hbar$ −curve and accelerate the convergence of the series. As depicted in Figure 6, the HAM solution without considering the second auxiliary parameter, can't give the correct solution. The comparison of amplitude oscillation between the HAM, HPM and numerical solution is shown in Table 1 and Figures 7-8. It is clear that the HAM results have the less error percentage than the numerical solution in compared with the HPM solution.

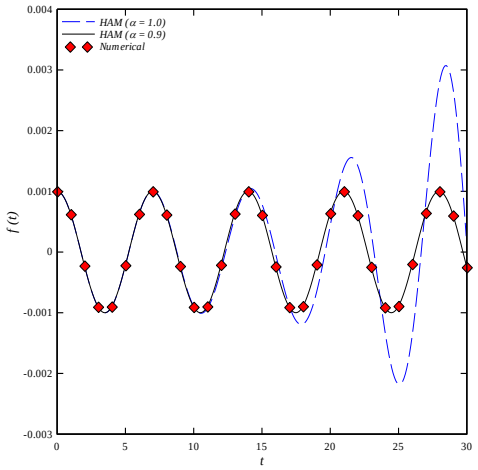

Figure 6. Comparison of amplitude oscillation for the HAM, HPM and numerical solution when $\nu = 0.3, r = 0.1, f(0) = 0.0002$ and $\alpha = 0.575$.

Table 1. Comparison of amplitude oscillation for the HAM, HPM and the numerical solution when$\nu = 0.3, r = 0.1, f(0) = 0.002$ and $\alpha = 0.575$.

t	Numerical	HPM	HAM	Numerical−HPM	Numerical− HAM
5	− 0.0019346	− 0.00193463	−0.00193461	2.58193×10^{-8}	1.80492×10^{-8}
10	−0.00174274	−0.00174279	−0.00174275	-4.84862×10^{-8}	-9.25511×10^{-9}
15	− 0.00143697	− 0.00143703	−0.00143694	5.84358×10^{-8}	-3.41738×10^{-8}
20	−0.00103727	−0.00103725	−0.00103722	-5.85421×10^{-8}	2.1476×10^{-8}
25	− 0.000569769	− 0.000569807	−0.000569766	4.80009×10^{-8}	-3.12375×10^{-9}
30	0.0000650315	−0.000065044	0.0000650314	-3.9926×10^{-8}	1.2389×10^{-10}

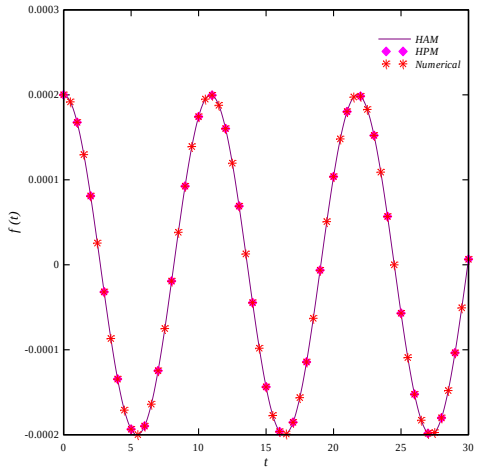

Figure 7. Comparison of amplitude oscillation for the HAM, HPM and numerical solution when $\nu = 0.3, r = 0.1, f(0) = 0.0002$ and $\alpha = 0.575$.

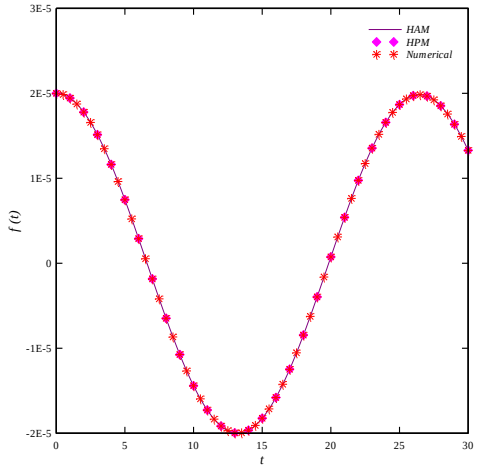

Figure 8. Comparison of amplitude oscillation for the HAM, HPM and numerical solution when $\nu = 0.3, r = 0.04, f(0) = 0.00002$, and $\alpha = 0.265$.

The effect of ν on amplitude oscillation is demonstrated in Figure 9 for the cases of $\nu = 0.1, 0.3$and 0.5. It should be noted that the amounts of second auxiliary parameter are equal to $0.325, 0.295$ and 0.325, respectively. Figure 10 displays the effect of r on amplitude oscillation for the cases of $r = 0.05, r = 0.1, r = 0.15$. The

values of second auxiliary parameter are equal to 0.285, 0.575 and 0.81, respectively. The influence of initial amplitude variation on amplitude oscillation is illustrated in Figure 11. The selected values of initial amplitude are equal to 0.0001 and0.0002. Figurs 12-17 depict the different mode shapes of oscillation for different values of physical parameters.

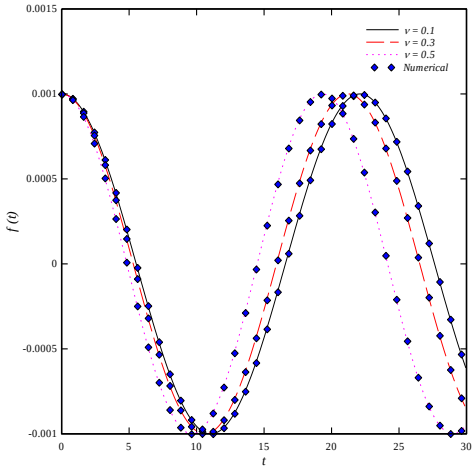

Figure 9. The effect of ν variation on amplitude oscillation when $r = 0.05$ and $f(0) = 0.001$.

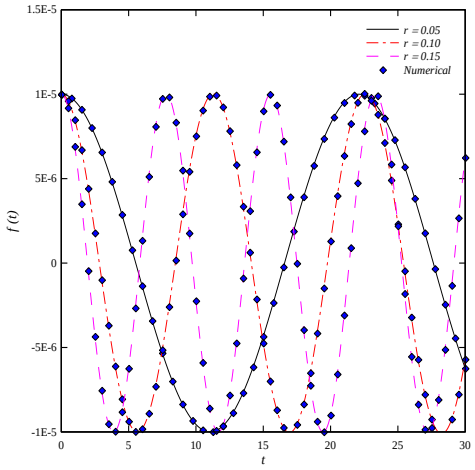

Figure 10. The effect of r variation on amplitude oscillation when $\nu = 0.1$ and $f(0) = 0.00001$.

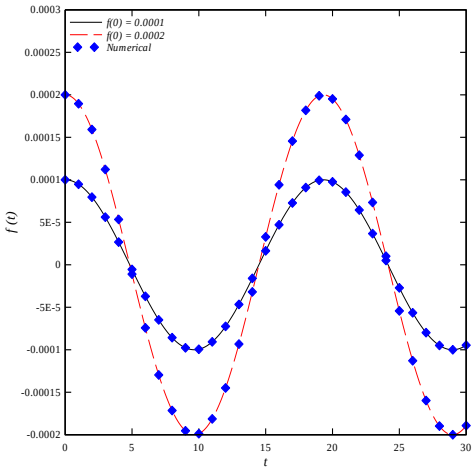

Figure 11. The effect of initial amplitude variation on amplitude oscillation when ν=0.5, r=0.05 and α=0.325.

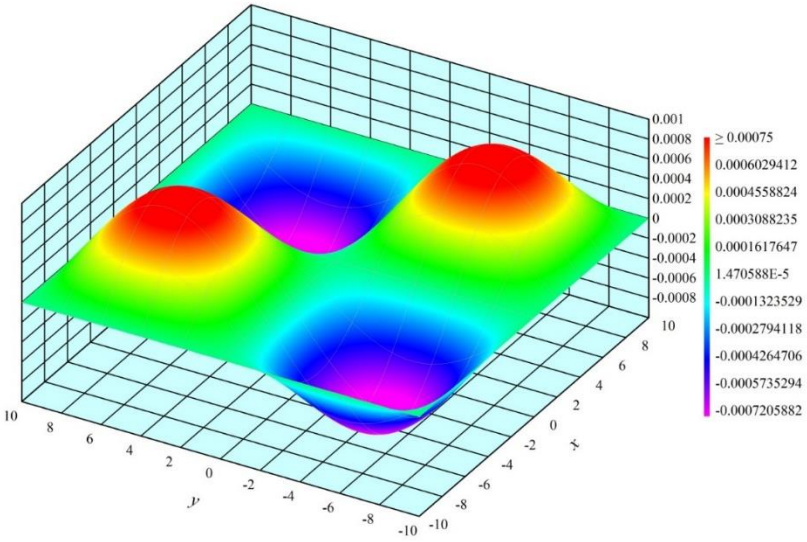

Figure 12. Different mode shape of oscillation for ν=0.05, r=0.15, $f0$=0.001, a=10, h=1, α=0.9 and t=25.

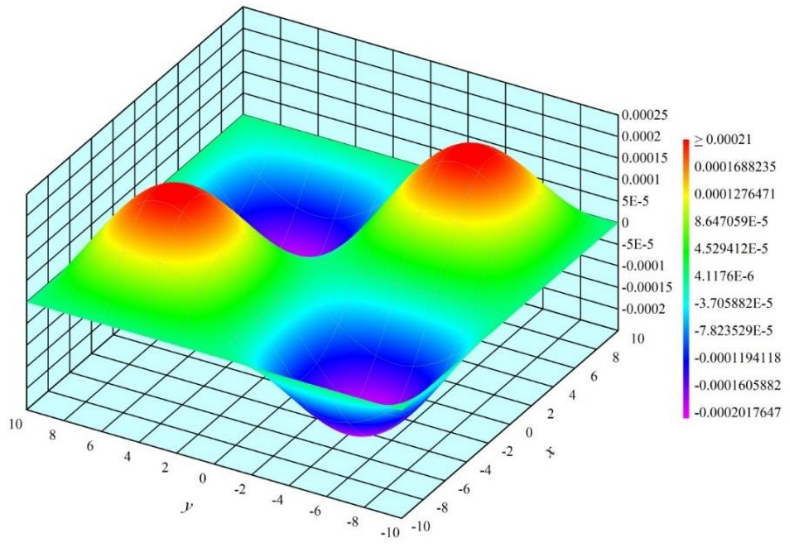

Figure 13. Different mode shape of oscillation for ν=0.05, r=0.15, $f0$=0.001, a=10, h=1, α=0.9 and t=5.

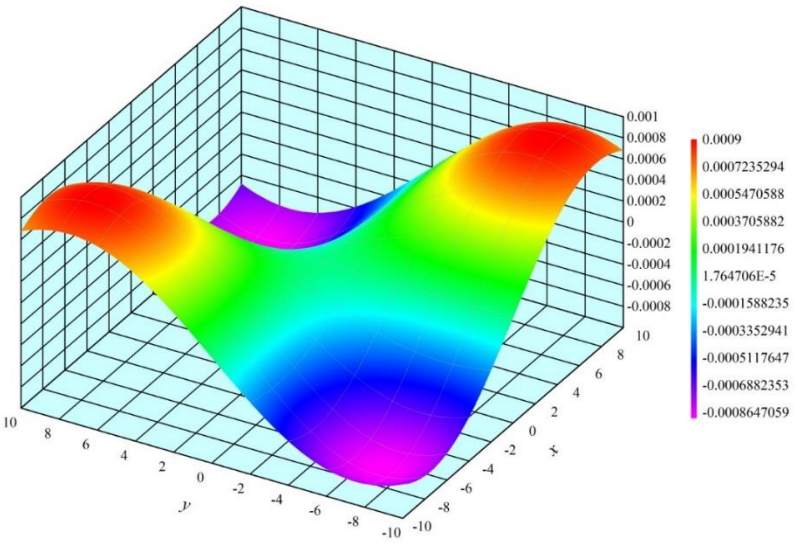

Figure 14. Different mode shape of oscillation for ν=0.05, r=0.15, $f0$=0.001, a=15, h=1, α=0.9 and t=10.

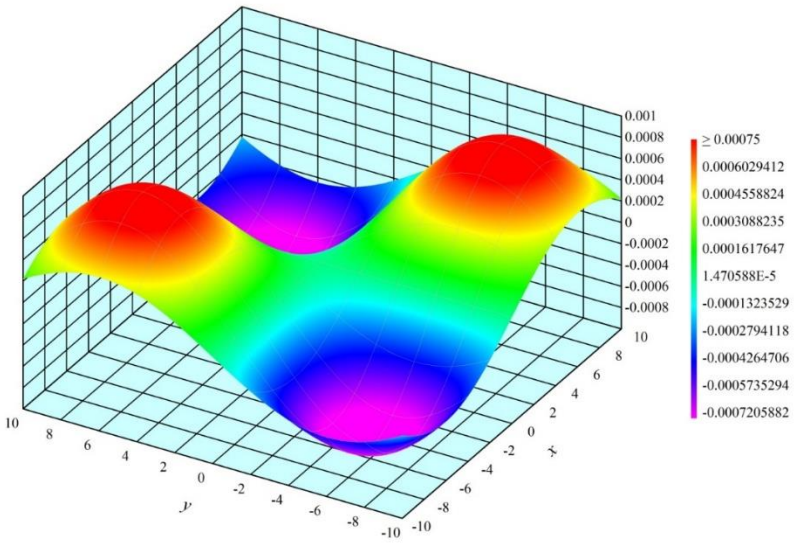

Figure 15. Different mode shape of oscillation for ν=0.05, r=0.15, $f0$=0.001, a=12, h=1, α=0.9 and t=25.

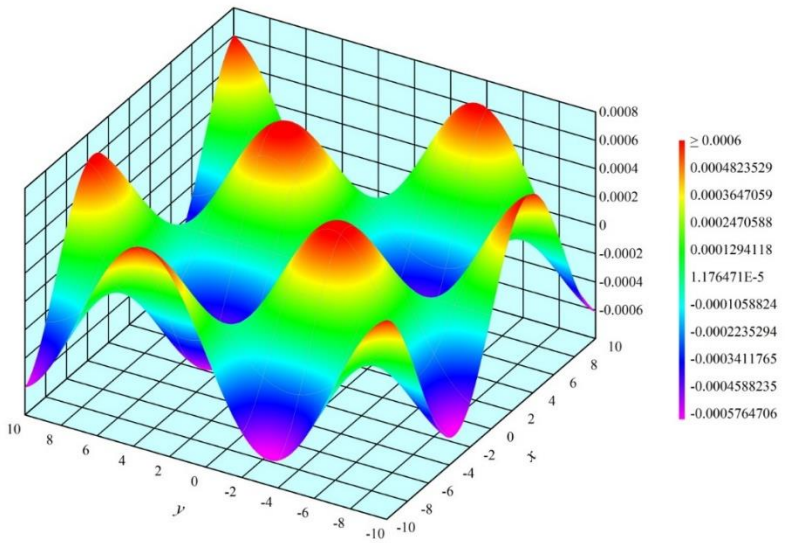

Figure 16. Different mode shape of oscillation for ν=0.05, r=0.15, $f0$=0.001, a=7, h=1, α=0.9 and t=20.

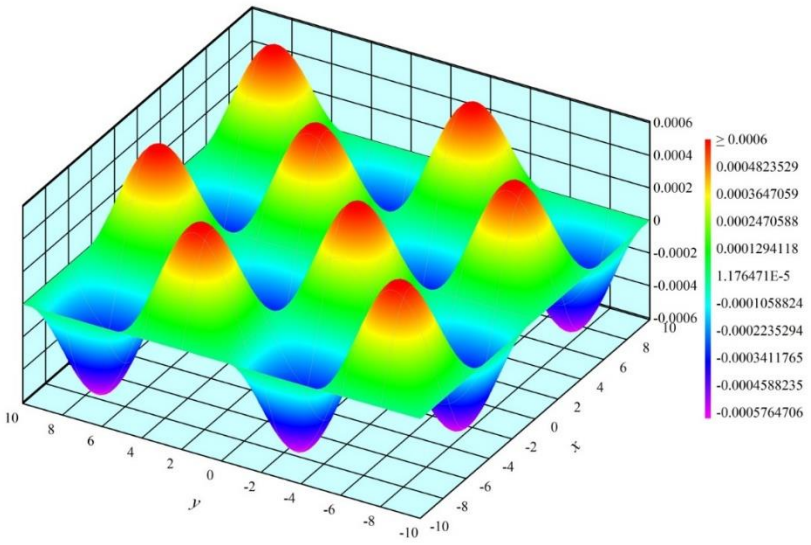

Figure 17. Different mode shape of oscillation for ν=0.05, r=0.15, $f0$=0.001, a=5, h=1, α=0.9 and t=15.

Conclusion

In the present study, the motion equations for an isotropic elastic plate in the presence of shear deformation and rotary inertia effects are derived in the form of the nonlinear differential equation with respect to time by the help of the Galrekin method. It is important to notice that this equation has nonlinearities in stiffness and inertia. In order to solve this ordinary nonlinear differential equation, the analytical method called HAM is employed. In this problem, due to high order of nonlinearities, the second auxiliary parameter is used to accelerate the convergences of the series. A comparison has been done between the HAM, HPM and numerical solution results. An excellent agreement can be seen between them. It should be mentioned that the HAM results have the less error percentage than the numerical solution in compared with the HPM solution. The HAM doesn't depend on any small physical parameter, despite the perturbation method. The effects of involved parameters such as $\boldsymbol{r}$, $\boldsymbol{\nu}$, initial amplitude on amplitude oscillation are checked and the different mode shapes of the oscillation for different physical parameters are illustrated.

Disclosure statement and funding

The authors declare no potential conflicts of interest. The present study received no financial support from any organization or institution.

Acknowledgment

We hereby express our gratitude and appreciation for the sincere cooperation of the management and experts of IPCO who cooperated in conducting tests and equipment and provided us with valuable information.

References

[1] Rashidi, M., Shooshtari, A., & Bég, O. A. (2012). Homotopy perturbation study of nonlinear vibration of Von Karman rectangular plates. *Computers & Structures*, *106*, 46–55.https://doi.org/10.1016/j.compstruc.2012.04.004

[2] Mahabadi, R. K., Shakeri, M., & Daneshpazhooh, M. (2016). Free Vibration of Laminated Composite Plate with Shape Memory Alloy Fibers. *Latin American Journal of Solids and Structures*, *13*(2), 314–330. https://doi.org/10.1590/1679-78252162

[3] Yazdi, A. A. (2016). Assessment of Homotopy Perturbation Method for Study the Forced Nonlinear Vibration of Orthotropic Circular Plate on Elastic Foundation. *Latin American Journal of Solids and Structures*, *13*(2), 243–256. https://doi.org/10.1590/1679-78252436

[4] Wang, Y.-G., Song, H.-F., Lin, W.-H., & Wang, J.-K. (2015). Large amplitude free vibration of micro/nano beams based on nonlocal thermal elasticity theory. *Latin American Journal of Solids and Structures*, *12*(10), 1918–1933. https://doi.org/10.1590/1679-78251904

[5] Huang, X.-L., & Shen, H.-S. (2005). Nonlinear free and forced vibration of simply supported shear deformable laminated plates with piezoelectric actuators. *International Journal of Mechanical Sciences*, *47*(2), 187–208. https://doi.org/10.1016/j.ijmecsci.2005.01.003

[6] Singha, M. K., & Daripa, R. (2007). Nonlinear vibration of symmetrically laminated composite skew plates by finite element method. *International Journal of Non-Linear Mechanics*, *42*(9), 1144–1152. https://doi.org/10.1016/j.ijnonlinmec.2007.08.001

[7] Huang, X.-L., & Shen, H.-S. (2004). Nonlinear vibration and dynamic response of functionally graded plates in thermal environments. *International Journal of Solids and Structures*, *41*(9–10), 2403–2427. https://doi.org/10.1016/j.ijsolstr.2003.11.012

[8] Kang, J.-H. (2003). Three-dimensional vibration analysis of thick, circular and annular plates with nonlinear thickness variation. *Computers and Structures*, *81*(16), 1663–1675. https://doi.org/10.1016/s0045-7949(03)00168-8

[9] Amabili, M. (2004). Nonlinear vibrations of rectangular plates with different boundary conditions: theory and experiments. *Computers and Structures*, *82*(31–32), 2587–2605. https://doi.org/10.1016/j.compstruc.2004.03.077

[10] Ye, Z. (1999). Application of Maple V to the nonlinear vibration analysis of circular plate with variable thickness. *Computers and Structures*, *71*(5), 481–488. https://doi.org/10.1016/s0045-7949(98)00302-2

[11] Shen, L., Shen, H.-S., & Zhang, C.-L. (2010). Nonlocal plate model for nonlinear vibration of single layer graphene sheets in thermal environments. *Computational Materials Science*, *48*(3), 680–685. https://doi.org/10.1016/j.commatsci.2010.03.006

[12] Belalia, S. A., & Houmat, A. (2012). Nonlinear free vibration of functionally graded shear deformable sector plates by a curved triangular p-element. *European Journal of Mechanics - A/Solids*, *35*(0), 1–9. https://doi.org/10.1016/j.euromechsol.2012.01.004

[13] Leung, A. Y. T., & Zhu, B. (2004). Geometric nonlinear vibration of clamped Mindlin plates by analytically integrated trapezoidal p-element. *Thin-Walled Structures*, *42*(7), 931–945. https://doi.org/10.1016/j.tws.2004.03.010

[14] Malekzadeh, P. (2007). A differential quadrature nonlinear free vibration analysis of laminated composite skew thin plates. *Thin-Walled Structures*, *45*(2), 237–250. https://doi.org/10.1016/j.tws.2007.01.011

[15] Nejati, M., Fard, K. M., Eslampanah, A., & Jafari, S. S. (2017). Free vibration analysis of reinforced composite functionally graded plates with steady state thermal conditions. *Latin American Journal of Solids and Structures*, *14*(5), 886–905. https://doi.org/10.1590/1679-78253705

[16] Yas, M. H., Nejati, M., & Jafari, S. S. (2017). Free Vibration of Functionally Graded Variable Thickness Carbon Nanotube Annular Plates [Research]. *Journal of Computational Methods In Engineering*, *35*(2), 131–158. https://doi.org/10.18869/acadpub.jcme.35.2.131

[17] Singh, B. N., & Lal, A. (2010). Stochastic analysis of laminated composite plates on elastic foundation: The cases of post-buckling behavior and nonlinear free vibration. *International Journal of Pressure Vessels and Piping*, *87*(10), 559–574. https://doi.org/10.1016/j.ijpvp.2010.07.013

[18] Abdulkerim, S., Dafnis, A., & Riemerdes, H.-G. (2019). Experimental Investigation of Nonlinear Vibration of a Thin Rectangular Plate. *International Journal of Applied Mechanics*, *11*(06), 1950059. https://doi.org/10.1142/s1758825119500595

[19] Chen, C.-S. (2007). The nonlinear vibration of an initially stressed laminated plate. *Composites Part B: Engineering*, *38*(4), 437–447. https://doi.org/10.1016/j.compositesb.2006.09.002

[20] Feli, S., Karami, L., & Jafari, S. S. (2019). Analytical modeling of low velocity impact on carbon nanotube-reinforced composite (CNTRC) plates. *Mechanics of Advanced Materials and Structures*, *26*(5), 394–406. https://doi.org/10.1080/15376494.2017.1400613

[21] Lo'pez-Puente, J., Zaera, R., & Navarro, C. (2007). An analytical model for high velocity impacts on thin CFRPs woven laminated plates. *International Journal of Solids and Structures*, *44*, 2837–2851. https://doi.org/10.1016/j.ijsolstr.2006.08.022

[22] Liao, S. J. (2004). *Beyond perturbation: introduction to the homotopy analysis method*. Chapman & Hall/CRC. http://books.google.com/books?id=AlUdMFes_JUC

[23] Liao, S. J. (2004). On the homotopy analysis method for nonlinear problems. *Applied Mathematics and Computation*, *147*(2), 499–513. https://doi.org/10.1016/S0096-3003(02)00790-7

[24] Marinca, V., Herişanu, N., & Nemeş, I. (2008). Optimal homotopy asymptotic method with application to thin film flow. *Open Physics*, *6*(3), 648–653. https://doi.org/10.2478/s11534-008-0061-x

[25] Yongqiang, L., Feng, L., & Dawei, Z. (2010). Geometrically nonlinear free vibrations of the symmetric rectangular honeycomb sandwich panels with simply supported boundaries. *Composite Structures*, *92*(5), 1110–1119. https://doi.org/10.1016/j.compstruct.2009.10.012

[26] M. Fooladi, S.R. Abaspour, A. Kimiaeifar, & M. Rahimpour. (2009). On the Analytical Solution of Kirchhoff Simplified Model for Beam by using of Homotopy Analysis Method. *World Applied Sciences Journal*, *6*, 297–302. https://doi.org/10.1590/1979-78276437

[27] Jafari, S. S., Rashidi, M. M., & Johnson, S. (2016). Analytical approximation of nonlinear vibration of euler-bernoulli beams. *Latin American Journal of Solids and Structures, an ABCM Journal*, *13*(7), 1250–1264. https://doi.org/10.1590/1679-78252437

[28] Ajam, H., Jafari, S. S., & Freidoonimehr, N. Analytical approximation of MHD nano-fluid flow induced by a stretching permeable surface using Buongiorno's model. *Ain Shams Engineering Journal*. http://dx.doi.org/10.1016/j.asej.2016.03.006

[29] Jafari, S. S., & Freidoonimehr, N. (2015). Second law of thermodynamics analysis of hydro-magnetic nano-fluid slip flow over a stretching permeable surface [journal article]. *Journal of the Brazilian Society of Mechanical Sciences and Engineering*, *37*(4), 1245–1256. https://doi.org/10.1007/s40430-014-0250-z

[30] Hoshyar, H., Ganji, D., Borran, A., & Falahati, M. (2015). Flow behavior of unsteady incompressible Newtonian fluid flow between two parallel plates via homotopy analysis method. *Latin American Journal of Solids and Structures*, *12*(10), 1859–1869. https://doi.org/10.1590/1679-78251807

[31] Bayat, M., Pakar, I., & Domairry, G. (2012). Recent developments of some asymptotic methods and their applications for nonlinear vibration equations in engineering problems: A review. *Latin American Journal of Solids and Structures*, *9*(2), 1–93. https://doi.org/10.1590/S1679-78252012000200003

[32] Kazemi, M. A., Jafari, S. S., Musavi, S. M., & Nejati, M. (2018). Analytical solution of convective heat transfer of a quiescent fluid over a nonlinearly stretching surface using Homotopy Analysis Method. *Results in Physics*, *10*, 164–172. https://doi.org/10.1016/j.rinp.2018.05.036

[33] Masoumnezhad, M., Kazemi, M., Askari, N., Taheri, M. H., & Ghamati, M. (2021). Semi-Analytical Solution of Unsteady Newtonian Fluid Flow and Heat Transfer between two Oscillation Plate under the Influence of a Magnetic Field. *Karafan Journal*, *18*(1), 35–62. https://doi.org/10.48301/kssa.2021.131037

[34] Askari, N., Salmani, H., Taheri, M. H., Masoumnezhad, M., & Kazemi, M. A. (2021). Heat transfer of water–graphene oxide nanofluid magnetohydrodynamic flow through a channel in the presence of the induced magnetic field. *Proceedings of the Institution of Mechanical Engineers, Part C: Journal of Mechanical Engineering Science*, *235*(11), 1966–1978. https://doi.org/10.1177/0954406220948902

[35] Aliakbar, V., Alizadeh-Pahlavan, A., & Sadeghy, K. (2009). The influence of thermal radiation on MHD flow of Maxwellian fluids above stretching sheets. *Communications in Nonlinear Science and Numerical Simulation*, *14*(3), 779–794. http://dx.doi.org/10.1016/j.cnsns.2007.12.003

[36] Alizadeh-Pahlavan, A., Aliakbar, V., Vakili-Farahani, F., & Sadeghy, K. (2009). MHD flows of UCM fluids above porous stretching sheets using two-auxiliary-parameter homotopy analysis method. *Communications in Nonlinear Science and Numerical Simulation*, *14*(2), 473–488. https://doi.org/10.1016/j.cnsns.2007.09.011

[37] Nourbakhsh, S. H., Pasha Zanoosi, A. A., & Shateri, A. R. (2011). Analytical solution for off-centered stagnation flow towards a rotating disc problem by homotopy analysis method with two auxiliary parameters. *Communications in Nonlinear*

Science and Numerical Simulation, *16*(7), 2772–2787. https://doi.org/10.1016/j.cnsns.2010.10.018

[38] Chia, C. (1980). *Nonlinear analysis of plates*. McGraw- Hill. https://www.abebooks.com/9780070107465/Nonlinear-Analysis-Plates-Chia-Chuen-Yuan-0070107467/plp